Neurotoxicology 94 (2023) 98–107

Contents lists available at ScienceDirect

Neurotoxicology

journal homepage: www.elsevier.com/locate/neuro

Receptor protein tyrosine phosphatase β/ζ regulates loss of neurogenesis in the mouse hippocampus following adolescent acute ethanol exposure

Milagros Galán-Llario [a], María Rodríguez-Zapata [a], Esther Gramage [a,c], Marta Vicente-Rodríguez [a,c], Teresa Fontán-Baselga [a], María Carmen Ovejero-Benito [a], Carmen Pérez-García [a,c], Javier Carrasco [a], Marco Moreno-Herradón [a], Julio Sevillano [b], María Pilar Ramos-Álvarez [b], José María Zapico [b], Beatriz de Pascual-Teresa [b], Ana Ramos [b], Gonzalo Herradón [a,c,*]

[a] Departamento de Ciencias Farmacéuticas y de la Salud, Facultad de Farmacia, Universidad San Pablo-CEU, CEU Universities, Urbanización Montepríncipe, Boadilla del Monte, 28668 Madrid, Spain
[b] Departamento de Química y Bioquímica, Facultad de Farmacia, Universidad San Pablo-CEU, CEU Universities, Urbanización Montepríncipe, Boadilla del Monte, 28668 Madrid, Spain
[c] Instituto de Estudios de las Adicciones, Universidad San Pablo-CEU, CEU Universities, Campus Montepríncipe, Alcorcón, 28925 Madrid, Spain

ARTICLE INFO

Keywords:
Alcohol
Neurotoxicity
Neuroinflammation
Pleiotrophin

ABSTRACT

Adolescence is a critical period for brain maturation in which this organ is more vulnerable to the damaging effects of ethanol. Administration of ethanol in mice induces a rapid cerebral upregulation of pleiotrophin (PTN), a cytokine that regulates the neuroinflammatory processes induced by different insults and the behavioral effects of ethanol. PTN binds Receptor Protein Tyrosine Phosphatase (RPTP) β/ζ and inhibits its phosphatase activity, suggesting that RPTPβ/ζ may be involved in the regulation of ethanol effects. To test this hypothesis, we have treated adolescent mice with the RPTPβ/ζ inhibitor MY10 (60 mg/kg) before an acute ethanol (6 g/kg) administration. Treatment with MY10 completely prevented the ethanol-induced neurogenic loss in the hippocampus of both male and female mice. In flow cytometry studies, ethanol tended to increase the number of NeuN+/activated Caspase-3+ cells particularly in female mice, but no significant effects were found. Ethanol increased Iba1+ cell area and the total marked area in the hippocampus of female mice, suggesting sex differences in ethanol-induced microgliosis. In addition, ethanol reduced the circulating levels of IL-6 and IL-10 in both sexes, although this reduction was only found significant in males and not affected by MY10 treatment. Interestingly, MY10 alone increased the total marked area and the number of Iba1+ cells only in the female hippocampus, but tended to reduce the circulating levels of TNF-α only in male mice. In summary, the data identify a novel modulatory role of RPTPβ/ζ on ethanol-induced loss of hippocampal neurogenesis, which seems unrelated to glial and inflammatory responses. The data also suggest sex differences in RPTPβ/ζ function that may be relevant to immune responses and ethanol-induced microglial responses.

1. Introduction

Adolescent drinking is a serious public health problem globally, with 6200 adolescents each day that initiated alcohol use in the past year (2019 National Survey on Drug Use and Health). More adolescent girls report alcohol use and binge drinking than boys. Binge drinking is a common pattern of consumption during this period of life, which is considered the most harmful drinking for the developing brain. In 2019, around 10% of 16–17 years old engaged in binge drinking in the past month in the United States. Binge drinking also contributes to an increased risk of developing alcohol use disorder. Up to 1.7% of adolescents aged 12–17 showed an alcohol use disorder during the previous year (2019 National Survey on Drug Use and Health). Thus, it is crucial to implement strategies during early adolescence to prevent the development of alcohol use disorder and brain damage.

Excessive alcohol consumption exerts several detrimental effects in the brain, contributing to neurodegeneration and neuroinflammation (Pascual et al., 2021). Adolescence is a critical period for the maturation of the brain during which highly plastic and dynamic processes participate in a variety of areas like the hippocampus (Lisdahl et al., 2013;

* Correspondence to: Lab. Pharmacology Faculty of Pharmacy, Universidad CEU San Pablo Urb. Montepríncipe, Boadilla del Monte, 28668 Madrid, Spain.
E-mail address: herradon@ceu.es (G. Herradón).

https://doi.org/10.1016/j.neuro.2022.11.008
Received 14 June 2022; Received in revised form 3 November 2022; Accepted 14 November 2022
Available online 17 November 2022

Yttri et al., 2004). During this stage of development, the brain is more vulnerable to the damaging effects of alcohol. For example, intermittent ethanol access in adolescent rats results in significant deficits in neurogenesis in the dentate gyrus, which is attributed to an excessive activation of the neuroimmune response and neuroinflammation that ends up causing the death of neuronal precursors by apoptosis (Swartzwelder et al., 2019). Alcohol activates the signaling pathway of toll-like receptor-4 (TLR4) in glial cells and contributes to the release of cytokines and pro-inflammatory mediators, which amplifies the neuroinflammatory response and the resulting brain damage (Pascual et al., 2018). The harmful effects of alcohol during adolescence differ significantly between sexes, being more accentuated in women (Guerri and Pascual, 2019; Orio et al., 2018). Consequently, understanding the factors that can prevent or restore alcohol-induced neuroinflammatory processes and developmental deficits in the adolescent brain is key.

Pleiotrophin (PTN) is a cytokine that is expressed in all species and is evolutionarily highly conserved (Papadimitriou et al., 2022). PTN is upregulated in the brain after the administration of different drugs of abuse, including alcohol (Herradón and Pérez-García, 2014; Vicente-Rodriguez et al., 2014), suggesting that PTN may regulate alcohol effects. Accordingly, it has been shown that the conditioning effects of alcohol are significantly increased in *Ptn*$^{-/-}$ mice, whereas the transgenic overexpression of PTN in the mouse brain blocks the rewarding effects of this drug (Vicente-Rodriguez et al., 2014). It is important to note that PTN modulates the immune response and neuroinflammation induced by different stimuli including amphetamine administrations (Herradon et al., 2019; Vicente-Rodríguez et al., 2016) and LPS-induced endotoxemia (Fernández-Calle et al., 2017).

Pleiotrophin is an endogenous inhibitory ligand of Receptor Protein Tyrosine Phosphatase (RPTP) β/ζ (Meng et al., 2000). The long and short isoforms of this receptor are found in humans and mice (Herradon et al., 2019; Nagai et al., 2022). Both have a transmembrane domain, but the RPTPβ/ζ-short isoform lacks a juxtamembrane extracellular region. In mice, a soluble RPTPβ/ζ isoform, named phosphacan, is also present (Nagai et al., 2022). This receptor is involved in the differentiation of oligodendrocytes (Lamprianou et al., 2011) and in the neuroimmune response in the adult brain (Harroch et al., 2002). Importantly, RPTPβ/ζ is mainly expressed in the central nervous system (CNS) in important areas for alcohol effects, such as the PFC, amygdala, or hippocampus (Cressant et al., 2017). Pleiotrophin induces the dimerization of RPTPβ/ζ, inhibiting as a result its phosphatase activity (Meng et al., 2000). This causes an increase in the levels of phosphorylation of its substrates (Pariser et al., 2005a, 2005b, 2005c), some of which play important roles in alcohol consumption such as Fyn kinase (Ron and Berger, 2018) and anaplastic lymphoma kinase (ALK) (Dutton et al., 2017).

Recently, through a rational drug development program, we designed and synthesized MY10, a blood-brain barrier (BBB)-permeable selective inhibitor of RPTPβ/ζ (Pastor et al., 2018). MY10 interacts with the intracellular domain PD1 of RPTPβ/ζ and inhibits its tyrosine phosphatase activity, thus mimicking the inhibitory action of PTN on this receptor (Pastor et al., 2018). In this manner, the systemic administration of MY10 reduces alcohol consumption and blocks the rewarding effects of alcohol in mice and rats (Calleja-Conde et al., 2020; Fernández-Calle et al., 2019, 2018b), replicating the effects obtained in mice with transgenic *Ptn* overexpression in the brain (*Ptn*-Tg) (Vicente-Rodriguez et al., 2014). Furthermore, LPS-induced microglial response was potentiated in mice treated with MY10 (Fernández-Calle et al., 2020), as it was previously observed in *Ptn*-Tg mice (Fernández-Calle et al., 2017). In addition, using MY10, we recently described that RPTPβ/ζ is important in neuronal and microglial viability and plays a role in the modulation of the neuroprotective phenotype of microglia and in the communication microglia-neuron (Del Campo et al., 2021). Therefore, we hypothesize that RPTPβ/ζ may also be involved in the regulation of the effects of alcohol on the adolescent brain.

2. Materials and methods

2.1. Animals

Male and female C57BL/6J mice of 5–6 weeks of age (15–22 g) were used. Mice were housed under controlled environmental conditions (22 ± 1 ºC and a 12-h light/12-h dark cycle) with free access to food and water. All the animals used in this study were maintained in accordance with European Union Laboratory Animal Care Rules (2010/63/EU directive) and protocols were approved by the Animal Research Committee of USP-CEU (authorization reference: PROEX 76.0/20). Animal studies were carried out in compliance with the ARRIVE guidelines.

2.2. Treatments

The RPTPβ/ζ inhibitor MY10 was synthesized as previously described (Pastor et al., 2018). Female and male mice were administered with 60 mg/kg MY10 or vehicle (10% dehydrated ethanol, 20% polysorbate 80, 70% PEG- 300) by oral gavage in a volume of approximately 0.1 ml one hour before a single i.p. injection of ethanol (6 g/kg, 25% v/v) or saline (control). This dose of ethanol was chosen to achieve in mice Blood Ethanol Concentrations (BECs) relevant to those found in human adolescents with a massive ingestion of ethanol (peak blood concentration, 700–750 mg/dL) (Pruett et al., 2020; Wiener et al., 2013). No mortality was observed after this ethanol treatment and all animals were fully recovered at the time of sacrifice, 18 h after ethanol administration. The dose and systemic route of administration of MY10 have been selected based on previous studies with this compound, in which dose-response curves show that the mean dose of 60 mg/kg reduces alcohol consumption in rodents and provides good bioavailability and BBB penetration (Calleja-Conde et al., 2020; Fernández-Calle et al., 2018b; Pastor et al., 2018). Blood samples (20 μl) were collected 1 h after the administration of ethanol (or saline) in heparinized capillary tubes. BECs (n = 4–5/group/sex) were determined using a nicotinamide adenine dinucleotide-alcohol dehydrogenase enzymatic assay (Zapata et al., 2006).

Animals were sacrificed 18 h after ethanol or saline administration (n = 5–6/group/sex). For immunohistochemistry analysis, animals were perfused with 4% p-formaldehyde. For flow cytometry analysis, animals were decapitated and hippocampus were rapidly removed and frozen in dry ice and stored to − 80 ºC until the procedures.

2.3. Immunohistochemistry

Thirty-μm sections of PFC, amygdala and hippocampus were obtained using a sliding microtome (Leica SM2010 R). Immunohistochemistry studies were performed in one slice per 120 μm in the case of the PFC (from the bregma 3.08 to –2.46 mm), in one slice per 360 μm in the case of the amygdala (from the bregma −0.82 to −2 mm), and in one slice per 360 μm for dentate gyrus (DG) (from the bregma −2.12 to −3.8 mm). To study neurogenesis, DG sections were incubated overnight with rabbit anti-doublecortin (DCx, Cell Signaling Technology, Danvers, MA, USA; 1:1000) antibody. After careful washing, sections were incubated with the biotinylated secondary antisera (Vector, Burlingame, CA, USA) at room temperature. The avidin-biotin reaction was performed using a Vectastain Elite ABC peroxidase kit. Immunoreactivity was visualized using 0.06% diaminobenzidine and 0.03% H_2O_2 diluted in PBS. Sections were mounted on gelatin/chrome alum-coated slides and photomicrographs were captured with the Leica SCN400 Scan Scanner (Leica, Solms, Germany).

To study glial responses, sections were incubated overnight at 4 °C with anti-glial fibrillary acidic protein (GFAP; Millipore, Madrid, Spain; 1:1000) and anti-ionized calcium-binding adaptor molecule 1 (Iba1, Wako, Osaka, Japan; 1:1000) antibodies, following by 30-min incubation with the Alexa-Fluor-555 and Alexa-Fluor-488 corresponding secondary antibodies (Invitrogen, Waltham, MA, USA; 1:500).

Photomicrographs were captured with a digital camera coupled to an optical microscope (DM5500B, Leica, Solms, Germany) using the LAS X Core software (Leica Microsystems, Wetzlar, Germany; offline version).

2.4. Image analysis

Analysis was performed using ImageJ/Fiji software (NIH, Bethesda, MD, USA, Version 1.50 f) on three photographs of each area from every subject. For DCx analysis, 490 × 277 μm standardized areas were used. Cell shape definition was improved by using the "Band Pass Filter" option before turning the image to 8-bit grayscale and using a "sharp" mask. DCx+ cells were counted in the subgranular zone (SGZ) of the DG, which was manually outlined. The outlined length was determined (mm) and cell density was calculated by dividing the number of DCx+ cells by the SGZ length (DCx+ cells/mm).

In the case of Iba1 and GFAP analysis, 640 × 480 μm standardized areas were used. After converting the images to 8-bit grayscale, the contrast was automatically enhanced, and images were despeckled and sharpened to better fit the cellular shape. Thresholds were adjusted using an automatic iterative method provided by ImageJ software to generate images with a maximum of Iba1+ or GFAP+ cells and a minimum of background artifacts. Total GFAP+ or Iba1 + marked area and cell count were then analyzed. In addition, morphology of individual Iba1+ cells was tested using the "Analyze Particle" function to measure cell area, perimeter, and circularity, as previously described (Fernández-Calle et al., 2017).

2.5. Cell nuclei isolation and flow cytometry

Cell nuclei isolation from hippocampus was carried out following previously established protocols with minor modifications (López-Sánchez et al., 2017; López-Sánchez and Frade, 2013). Briefly, each mouse hippocampus was disaggregated in a Dounce homogenizer in 3.0 ml ice-cold, PBS 0.1% Triton (PBT) containing protease inhibitor cocktail (Roche, Basilea, Switzerland). Undissociated tissue was discarded by centrifugation at 200 g for 1.5 min at 4 ºC. Supernatants were collected in 40 ml of PBT. Pellets were washed with PBT and centrifuged at 100 g for 2 min at 4 ºC.

Supernatants were added to the previous ones and centrifuged at 400 g for 4 min at 4 ºC. Precipitated nuclei were incubated in 250 μl cold PBT for at least 20 min at 4 ºC. Anti-NeuN (Abcam (ab134014), Cambridge, United Kingdom; 1:62), anti-cleaved Caspase-3 (Cell Signaling Technology (Asp175,5A1), Danvers, MA, USA; 1:192), donkey anti-chicken IgY Alexa Fluor 488 (Jackson Immuno Research Labs (703−545−155), Baltimore, PA, USA; 1:417) and goat anti-Rabbit IgG (H+L), DyLight 405 (Invitrogen (33550), Waltham, MA, USA; 1:357) antibodies, 1/17 fetal calf serum (Thermo Fisher Scientific Inc., Waltham, MA, USA) and 1.2 mg/ml BSA (Sigma Aldrich, San Luis, MO, USA) were added simultaneously to the nuclei. Fluorescence minus one controls were prepared discarding one of the primary antibodies. The reaction was incubated O/N at 4 ºC in the dark. Immunostained nuclei were filtered through a 40-μm nylon filter (ClearLine, Cultek, Madrid, Spain) and volume was adjusted to 350 μl (controls)− 600 μl (samples) with PBT. Samples were analyzed in an Attune™ NxT Acoustic Focusing Cytometer (Thermo Fisher Scientific Inc., Waltham, MA, USA) in the flow cytometry Unit of "Instituto de Medicina Molecular Aplicada" (IMMA, Universidad San Pablo CEU). The flow cytometer was equipped with a violet (405-nm), a blue (488-nm) and a red laser (638-nm). The emission filters used were BP 530/30 (BL1) for Alexa 488 and BP 440/50 for DyLight 405 (VL1). Samples were analyzed at a flow rate of 100 μl/min.

Data were analyzed and compensated with the Attune™ TxT software (Thermo Fisher Scientific Inc., Waltham, MA, USA) and displayed using logarithmic scaling. Singlet cells were identified in the diagonal of a dot plot of forward scatter (FSC) pulse height vs. FSC pulse area. To normalize data between experiments, % NeuN+ , % activated Caspase 3+ or % NeuN+ /activated caspase 3+ from singlets of each individual were referred to values of the male controls (vehicle+saline) of each experiment. Each experiment was repeated at least 4 times.

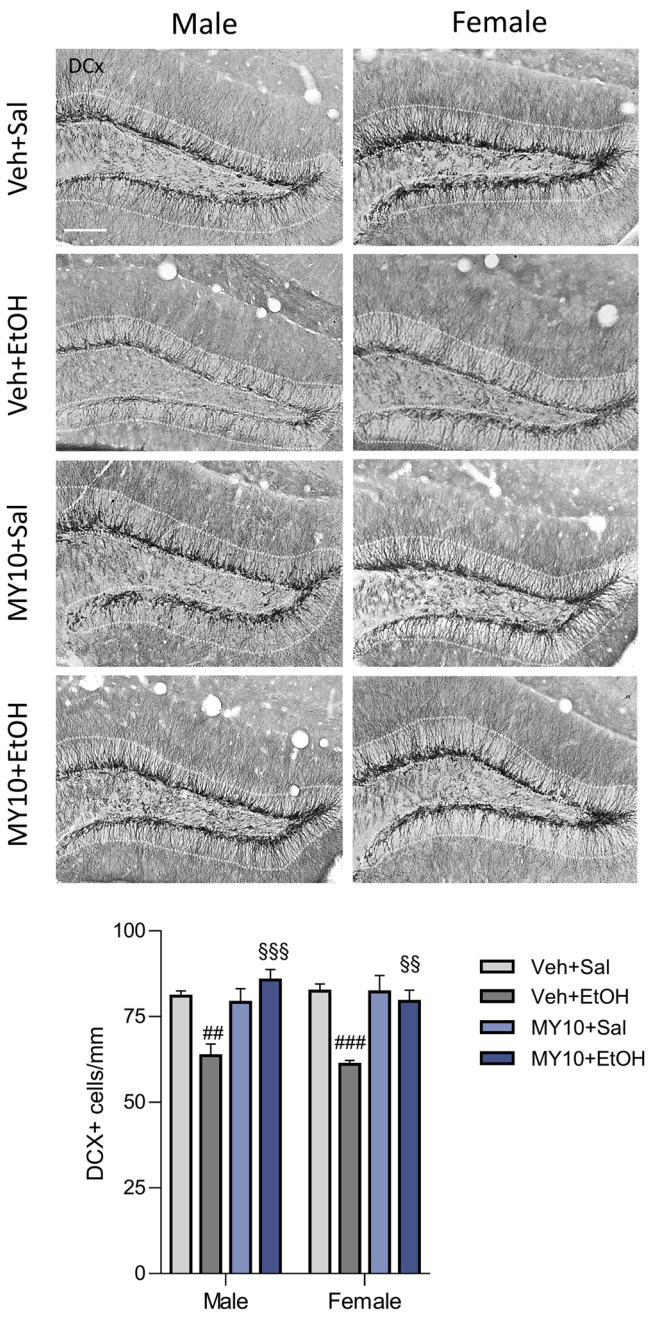

Fig. 1. Effects of MY10 on ethanol-induced decrease of neural progenitor cells in the adolescent hippocampus. Photomicrographs are from doublecortin (DCX)-immunostained hippocampal sections of vehicle+saline (Veh+Sal)-, vehicle+ethanol (Veh+EtOH)-, MY10 +saline (MY10 +Sal)- and MY10 +ethanol (MY10 +EtOH)-treated animals (n = 5/group). Dashed lines indicate the outline of the granule cell layer of the hippocampal dentate gyrus. The graph represents quantification of data obtained from the counts of DCX+ cells/mm in dentate gyrus sections. ## $P < 0.01$; ### $P < 0.001$ vs. vehicle+saline within same sex. §§ $P < 0.01$; §§§ $P < 0.001$ vs. vehicle+ethanol within same sex. Scale bar = 200 μm.

2.6. Cytokine quantification

Circulating concentrations of cytokines were determined in 10 μl plasma samples extracted 1 h after the injection of ethanol or saline.

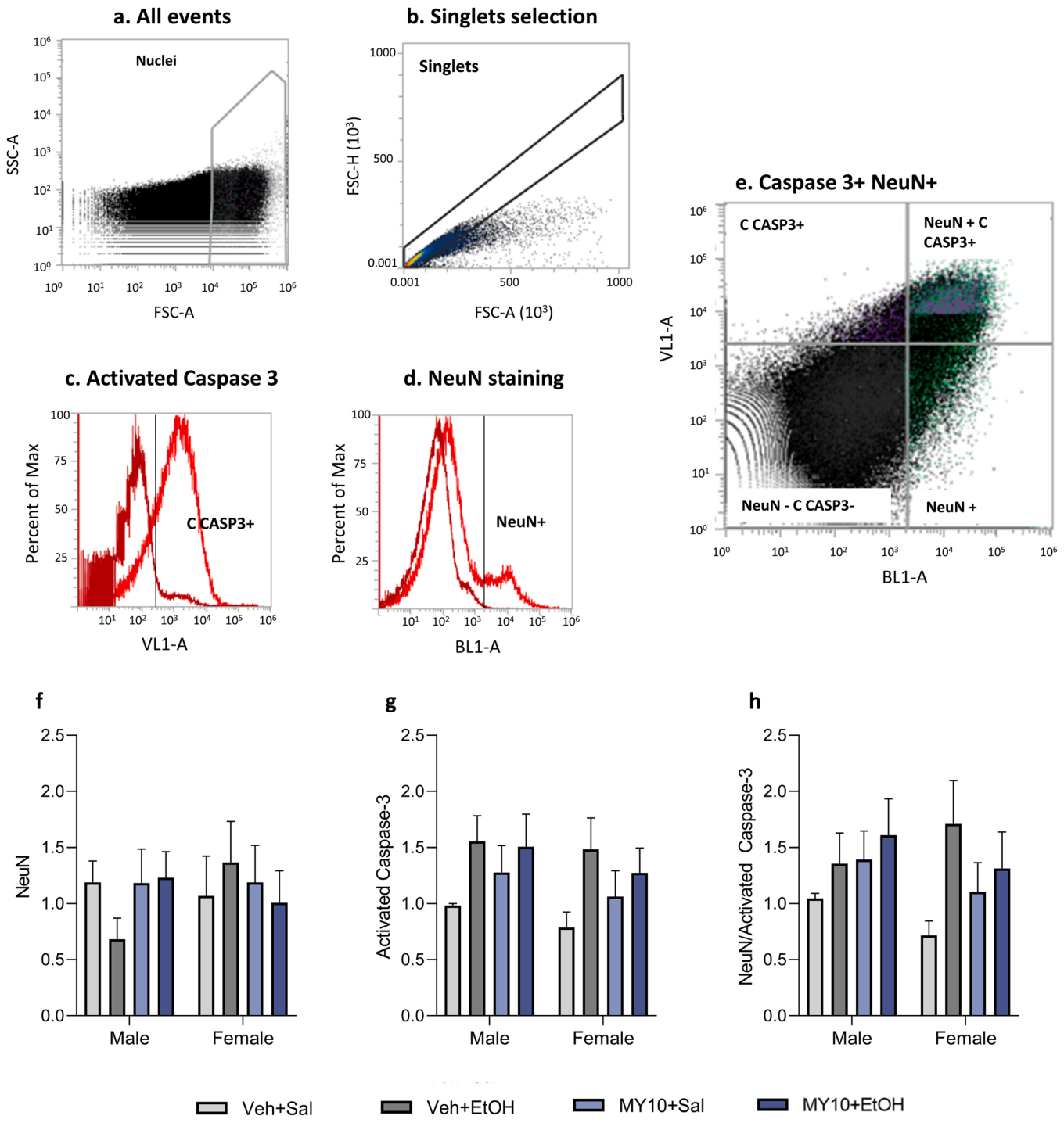

Fig. 2. Effects of MY10 and ethanol on neuronal apoptosis in the adolescent hippocampus. (a-d) Representative electronic gating procedure for nuclear samples of hippocampus analyzed by flow cytometry. (a) Cell nuclei population was gated on forward scattering area (FSC-A), a measure of the event size, and size scattering area (SSC-A) that represents event granularity or complexity. (b) Singlets were selected from the nuclei population by screening of the diagonal of forward scatter area (FSC-A) vs forward scatter height (FSC-H) plot. (c) Overlay histogram showing specific activated caspase 3 + staining detected with the VL1 filter in the singlets population. (d) Overlay histogram showing specific NeuN+ staining detected with the BL1 filter in the singlets population. (e) Double staining of singlets with VL1-A and BL1-A to find the double positive population for NeuN+ and active caspase-3. Abbreviations: C CASP3: activated/cleaved caspase 3. (f) NeuN+ population. (g) Activated caspase 3 + population. (h) NeuN+ and activated caspase 3 + population in the following groups: vehicle+saline (Veh+Sal)-, vehicle+ethanol (Veh+EtOH)-, MY10 +saline (MY10 +Sal)- and MY10 +ethanol (MY10 +EtOH)-treated animals (n = 4/group). To normalize data between experiments in figures f-h, % NeuN+ , % activated Caspase 3 + or % NeuN+ /activated caspase 3 + from singlets of each individual were referred to values of the male controls (vehicle+saline) of each experiment.

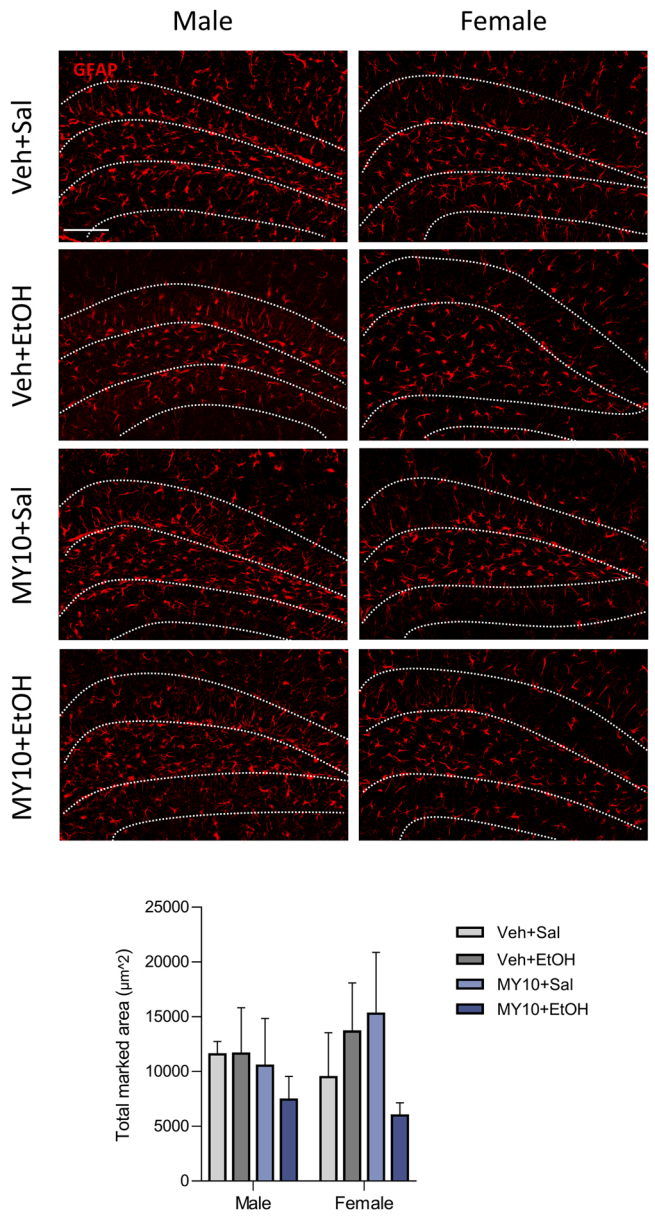

Fig. 3. Effects of MY10 on ethanol-induced astrocytic responses in the adolescent hippocampus. Photomicrographs are from GFAP-immunostained hippocampus sections of vehicle+saline (Veh+Sal)-, vehicle+ethanol (Veh+EtOH)-, MY10 +saline (MY10 +Sal)- and MY10 +ethanol (MY10 +EtOH)-treated animals (n = 5–6/group). Dashed lines indicate the outline of the granule cell layer of the hippocampal dentate gyrus. The graph represents the quantification of data (mean ± S.E.M) obtained from GFAPir proportional marked area in dentate gyrus sections. Scale bar = 100 µm.

Levels of tumor necrosis factor-α (TNF-α), interleukin 1β (IL-1β), interleukin 6 (IL-6), monocyte chemoattractant protein-1 (MCP-1), interleukin 4 (IL-4), and interleukin 10 (IL-10) were measured by multiplex luminometry (Beadlyte mouse multiplex cytokine detection system, MHSTCMAG-70 K, Merck Millipore, Spain) according to the manufacturer's description and protocols previously used by our group (Fernández-Calle et al., 2017).

2.7. Statistics

Data are presented as mean ± standard error of the mean (S.E.M.). Data were analyzed using two-way ANOVA considering sex and treatment as variants. Relevant differences were analyzed by post-hoc comparisons with Sidak's post-hoc tests. All statistical analyses were performed using Graph-Pad Prism program version 8 (San Diego, CA, USA).

3. Results

3.1. Inhibition of RPTPβ/ζ with MY10 prevents ethanol-induced loss of hippocampal neural progenitors in male and female mice

To test the possibility that RPTPβ/ζ may be involved in the regulation of ethanol-induced loss of neural progenitors in the DG, adolescent mice were treated with the RPTPβ/ζ inhibitor MY10 (60 mg/kg) 1 h before ethanol administration (6 g/kg). First, we measured BECs 1 h after ethanol administration in male and female mice pre-treated with MY10 or vehicle (control). Since ANOVA did not reveal significant sex differences, data from male and female mice within treatment were pooled to analyze possible changes in the BECs induced by MY10. We did not observe significant differences between treatments ($t = 0.2612$, $df = 14$; $P = 0.7978$) in animals pre-treated with vehicle or MY10 before ethanol administration (727 ± 90.3 mg/dl and 757.1 ± 82.8 mg/dl, respectively), confirming previous studies showing that MY10 did not exert significant effects on BECs in adult mice (Fernández-Calle et al., 2018b).

Sections of DG were immunostained with anti-DCX antibody. ANOVA revealed a significant effect of the treatment on the number of DCX+ cells ($F(3,38) = 16.72$; $P < 0.0001$, Fig. 1). Ethanol caused a significant reduction in the number of DCX+ cells in the DG of male and female mice (Fig. 1). Very interestingly, pre-treatment with MY10 completely blocked this effect of ethanol in both male and female mice, whereas treatment with MY10 alone (MY10 +Sal) did not have any effect on the number of DCX+ cells (Fig. 1). To explore the possibility that these effects of MY10 and ethanol are also observed in mature neurons, we analyzed the labeling for NeuN and activated caspase-3 in the hippocampus using flow cytometry (Fig. 2). ANOVA detected significant treatment-induced changes in activated caspase-3 labeling ($F(3, 25) = 3.282$; $P = 0.0374$, Fig. 2g) and a trend in the case of NeuN/activated Caspase-3 labeling ($F(3, 25) = 2.400$; $P = 0.0917$, Fig. 2h). Post-hoc analysis only revealed a robust trend of ethanol treatment to increase the number of NeuN/activated Caspase-3 cells in the hippocampus of female mice (Fig. 2h; $P = 0.072$). Pre-treatment with MY10 did not seem to have any relevant effects (Fig. 2).

3.2. Effects of inhibition of RPTPβ/ζ with MY10 and ethanol on glial and immune responses in male and female mice

To study the possibility of a correlation between the regulation of glial responses and loss of hippocampal neural progenitors, we studied astrocytic and microglial responses in immunohistochemistry studies in the DG. We did not observe significant effects of the treatment or the sex in the analysis of immunoreactive GFAP (GFAPir) in the hippocampus of male and female mice (Fig. 3).

However, we observed significant differences in the study of immunoreactive Iba1 (Iba1ir, Fig. 4). Immunostaining of DG sections with anti-Iba1 microglial antibody revealed significant differences between male and female mice in the total marked area ($F(1,37) = 31.29$; $P < 0.0001$, Fig. 4a), number of Iba1 + cells ($F(1,35) = 11.42$; $P = 0.002$, Fig. 4b) and cell area ($F(1,37) = 11.18$; $P = 0.002$, Fig. 4c). We also found a significant interaction sex x treatment in Iba1 + cell area ($F(3,37) = 3.064$; $P = 0.039$; Fig. 4c), and a robust trend of a significant effect of the sex in the perimeter ($F(1,37) = 4.079$; $P = 0.051$, Fig. 4d). We did not find significant sex differences in circularity (Fig. 4e). Post-hoc comparisons revealed specific differences between sexes in groups treated with MY10 or with ethanol. Thus, ethanol-treated female mice showed a significant increase of the total marked area (Fig. 4a) and cell area (Fig. 4c), whereas female mice treated only with MY10 showed a significant increase of the total marked area

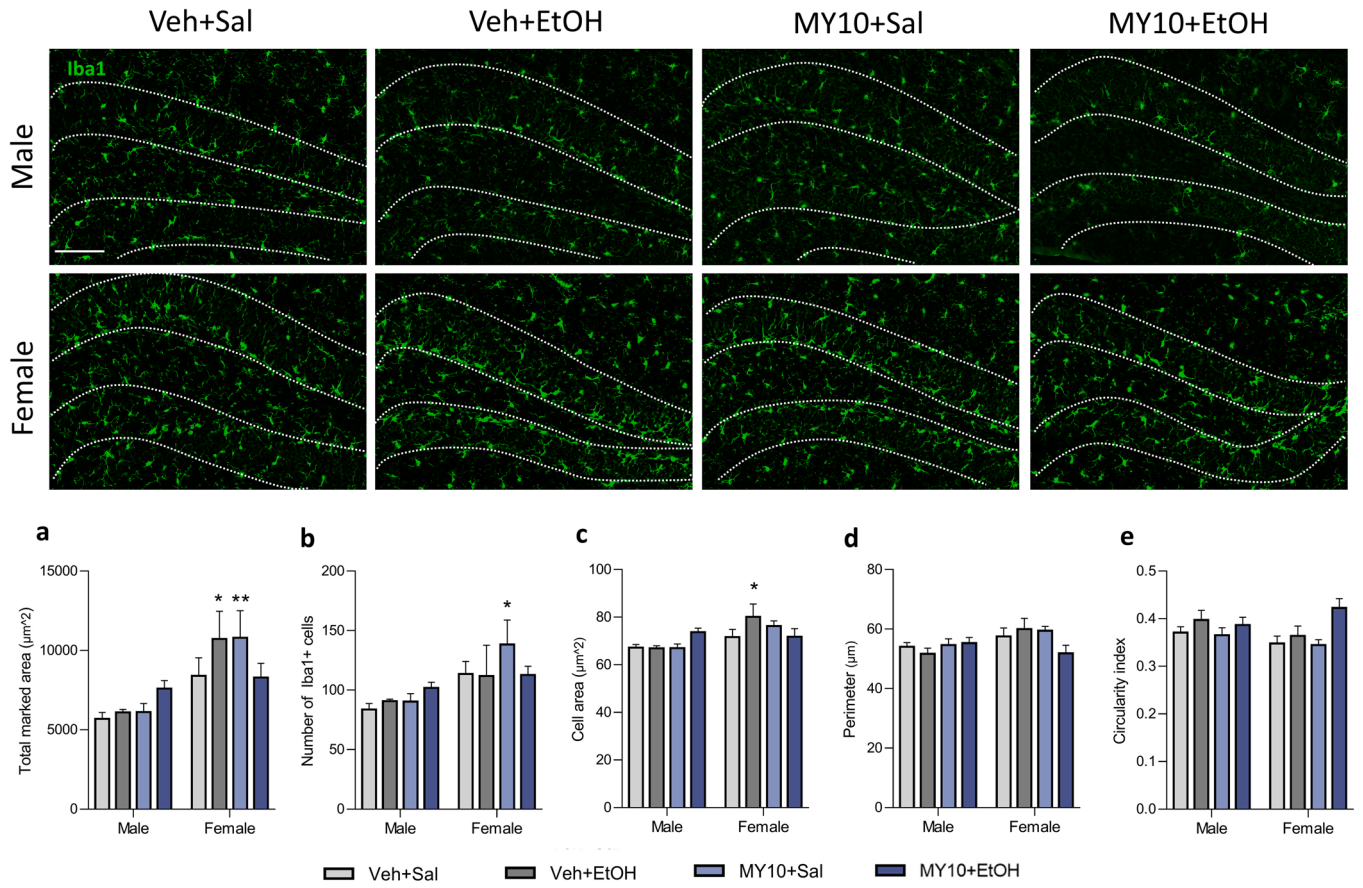

Fig. 4. Effects of MY10 on ethanol-induced microglial responses in the adolescent hippocampus. Photomicrographs are from Iba1-immunostained hippocampal sections of vehicle+saline (Veh+Sal)-, vehicle+ethanol (Veh+EtOH)-, MY10 +saline (MY10 +Sal)- and MY10 +ethanol (MY10 +EtOH)-treated animals (n = 4–5/group). Graphs represent quantification of data (mean ± S.E.M) obtained from (a) total marked area, (b) the counts of Iba1-positive cells, (c) cell area, (d) soma perimeter and (d) circularity index in dentate gyrus sections. Dashed lines indicate the outline of the granule cell layer of the hippocampal dentate gyrus. * $P < 0.05$; * * $P < 0.01$ vs. male mice with the same treatment. Scale bar = 100 µm.

(Fig. 4a) and the number of Iba1 + cells (Fig. 4b) compared to male mice with the same treatment. Regarding treatment-related differences, with the exception of circularity ($F(3,37) = 3.852$; $P = 0.017$, Fig. 4e), we did not detect significant effects of the treatment on any of the parameters measured that could correlate with the observed MY10 protection against ethanol-induced neural progenitors loss (Fig. 1).

Microglial cells were also studied in other brain regions that express RPTPβ/ζ and are important in the control of alcohol responses. Immunostaining of PFC sections with anti-Iba1 microglial antibody (Fig. 5) revealed significant differences between male and female mice in all parameters measured: total marked area ($F(1,37) = 14.57$; $P = 0.0005$, Fig. 5a), number of Iba1 + cells ($F(1,38) = 14.92$; $P = 0.0004$, Fig. 5b), cell area ($F(1,39) = 20.30$; $P < 0.0001$, Fig. 5c), perimeter ($F(1,39) = 12.66$; $P = 0.001$, Fig. 5d) and circularity ($F(1,39) = 14.15$; $P = 0.0006$, Fig. 5e). In a similar manner to hippocampus, female mice showed enhanced morphological parameters indicative of a more activated state of microglia. In contrast, significant changes due to treatment were only observed in the case of cell area ($F(3,39) = 2.958$; $P = 0.0441$, Fig. 5c). Post-hoc comparisons revealed specific differences between sexes in groups treated with MY10 and ethanol. Female mice that received this treatment showed a significant increase of the total marked area (Fig. 5a) and cell area (Fig. 5c), and a significant decrease of circularity (Fig. 5e) compared to male mice with the same treatment. On the other hand, Iba1ir in Basolateral Amygdala (BLA) and Central Amygdala (CeA) did not show significant sex-related differences (supplementary figure 1). We observed treatment-related differences in some of the morphological parameters measured, but Post-hoc comparisons did not reveal specific differences between treatments (supplementary figure 1).

To test the possibility that RPTPβ/ζ may be involved in the regulation of immune responses induced by ethanol, we also measured the circulating levels of different cytokines. We did not find significant sex- or treatment-related changes in the plasma concentrations of IL-1β, MCP-1 and IL-4 (Fig. 6a-c). However, ANOVA detected a significant effect of the treatment in the circulating levels of IL-6 ($F(3,49) = 9.106$; $P < 0.0001$, Fig. 6d) and IL-10 ($F(3,46) = 4.750$; $P = 0.0057$, Fig. 6e). Ethanol reduced the circulating levels of IL-6 and IL-10 in both sexes, although this reduction was only found significant in males. Pretreatment with MY10 did not cause any effect on ethanol-induced reduction of the levels of these cytokines (Fig. 6d,e). We also observed a significant interaction treatment x sex in the regulation of the levels of TNF-α ($F(3,50) = 2.871$; $P = 0.0455$, Fig. 6f). Post-hoc comparisons revealed a robust trend in the reduction of circulating levels of TNF-α caused by the treatment with MY10 alone (MY10 +Sal group) only in male mice ($P = 0.0547$, Fig. 6f).

4. Discussion

Hippocampal neurogenesis is a very active process during adolescence and is important for learning and memory processes (Snyder, 2019). Disruption of this process by binge ethanol exposure persists throughout adulthood (Broadwater et al., 2014). The long-term consequences, beyond the learning and memory deficits and early cognitive decline, may include an increased risk of developing neurodegenerative diseases as loss of neurogenesis is a hallmark of these disorders (Anacker and Hen, 2017; Winner and Winkler, 2015). Given that 90% of alcohol

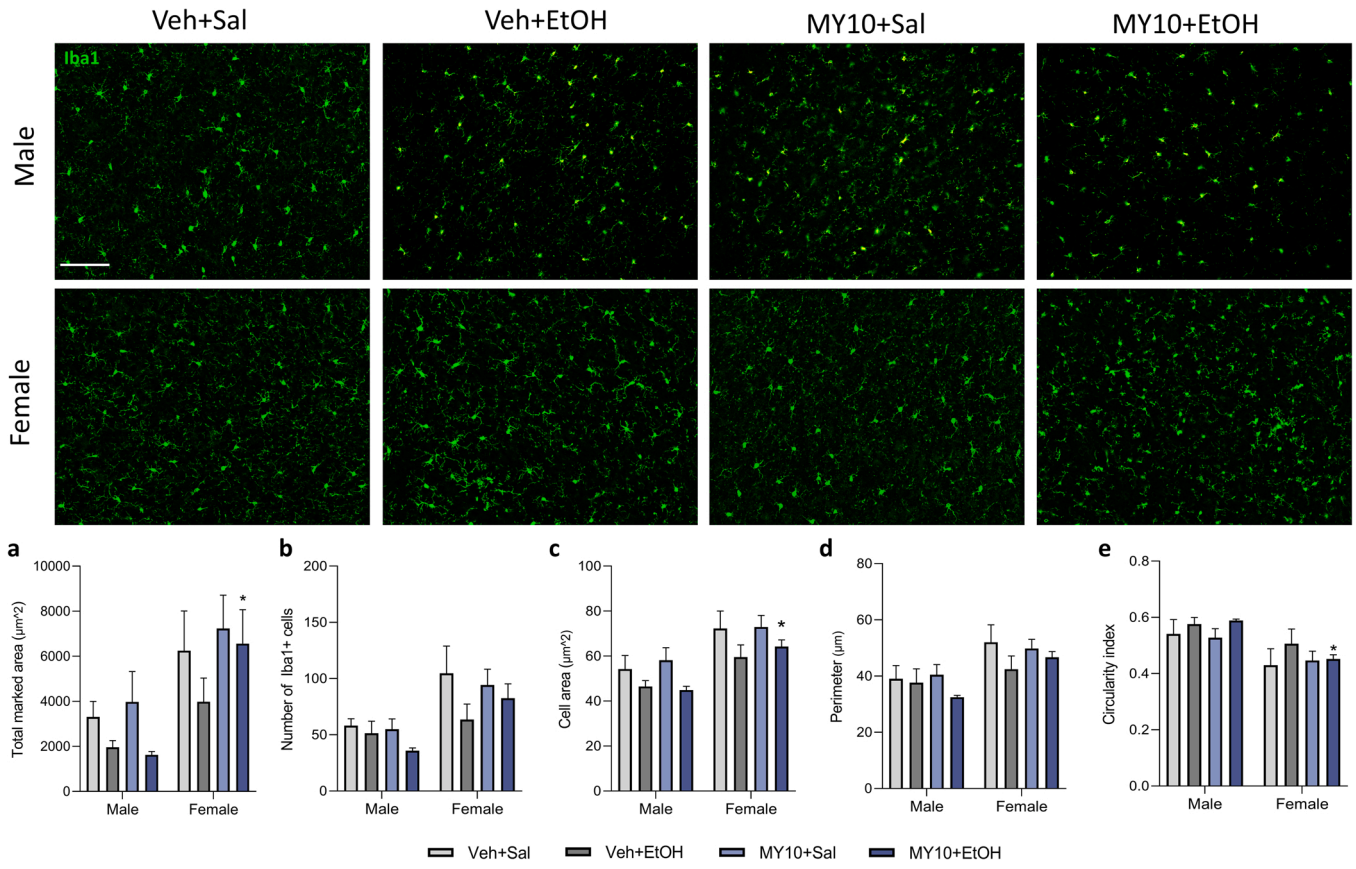

Fig. 5. Effects of MY10 on ethanol-induced microglial responses in the adolescent PFC. Photomicrographs are from Iba1-immunostained PFC sections of vehicle+saline (Veh+Sal)-, vehicle+ethanol (Veh+EtOH)-, MY10 +saline (MY10 +Sal)- and MY10 +ethanol (MY10 +EtOH)-treated animals (n = 4–5/group). Graphs represent quantification of data (mean ± S.E.M) obtained from total marked area (a), the counts of Iba1-positive cells (b), cell area (c), soma perimeter (d) and circularity index (e). * $P < 0.05$ vs. male mice with the same treatment. Scale bar = 100 µm.

consumed by adolescents is in the form of binge drinking, there is an urgent need to identify the molecular mechanisms underlying the loss of hippocampal neurogenesis caused by this drug. In the present work, we identify a novel mechanism of regulation of ethanol-induced decrease of adolescent hippocampal neurogenesis. We demonstrate that inhibition of RPTPβ/ζ prevents ethanol-induced loss of neurogenesis. In contrast, our data tend to discard relevant effects in mature neurons as ethanol did not cause significant changes in the percentage of NeuN+ cells in the hippocampus and only tended to increase the number of active caspase-3+ mature neurons, particularly in the case of female mice.

The data suggest a pivotal role of the PTN/RPTPβ/ζ axis in the regulation of ethanol-induced neurogenic loss. PTN is a neurotrophic factor whose levels of expression are upregulated in the mouse brain after an acute ethanol administration (Vicente-Rodriguez et al., 2014). PTN binds to different receptors to play different roles in physiological and pathological contexts. RPTPβ/ζ is one receptor thought to be key in the effects of PTN in the CNS (Herradon et al., 2019). Since PTN is an endogenous inhibitor of the phosphatase activity of RPTPβ/ζ (Herradon and Ezquerra, 2009; Meng et al., 2000), the present data suggest that upregulation of PTN in the brain after ethanol administration may take part of compensatory mechanisms to mitigate the neurotoxic effects of this drug.

Immune and glial responses to ethanol have been consistently linked to loss of hippocampal neurogenesis (Macht et al., 2020; Vetreno et al., 2018). In addition, the inflammatory response to ethanol underlies long-term behavioral alterations, psychiatric disorders and neurodegeneration related to excessive ethanol consumption (Coleman and Crews, 2018; Meredith et al., 2021; Pascual et al., 2015, 2021). PTN modulates LPS-induced microglial activation and neuroinflammation in the mouse brain (Fernández-Calle et al., 2020, 2018a, 2017), and inhibition of RPTPβ/ζ with MY10 results in potentiation of LPS-induced microglial responses, thus mimicking the effects of PTN (Fernández-Calle et al., 2020, 2017). This suggested that the PTN/RPTPβ/ζ axis could modulate the immune response in other contexts in which the expression of this neurotrophic factor is upregulated (i.e. after ethanol administration). Therefore, we tested the possibility that MY10 could modulate the glial and immune responses in adolescent mice treated with an acute dose of ethanol. In our studies, PFC and hippocampi of female mice showed enhanced morphological parameters of Iba1+ cells, compatible with a more activated state of microglia, independently of the treatment received. Sex differences in microglial state are known in the healthy brain and in conditions such as stress or neurodegeneration (Bilbo et al., 2012; Bollinger, 2021; Posillico, 2021) and are more evident in areas like PFC (Bollinger, 2021), where female rats show microglia with broadened morphology compatible with a surveillant phenotype. In this brain area, we found that these sex differences are more pronounced in animals treated with MY10 and ethanol.

In the hippocampus, we found only in female mice that ethanol increased the Iba1+ cell area and the total marked area, whereas treatment with MY10 alone increased the total marked area and the number of Iba1+ cells, again only in female mice. Together, these data are compatible with the idea of a sex-dependent ethanol-induced microgliosis in this brain area and suggest the possibility of a different RPTPβ/ζ functionality in male and female mice, which may be relevant to the modulation of microglial morphology. In addition, the data tend to discard that the protective effects of MY10 against ethanol-induced loss of hippocampal neurogenesis is related to modulation of glial responses in this brain area. All in all, it has to be noted that one limitation

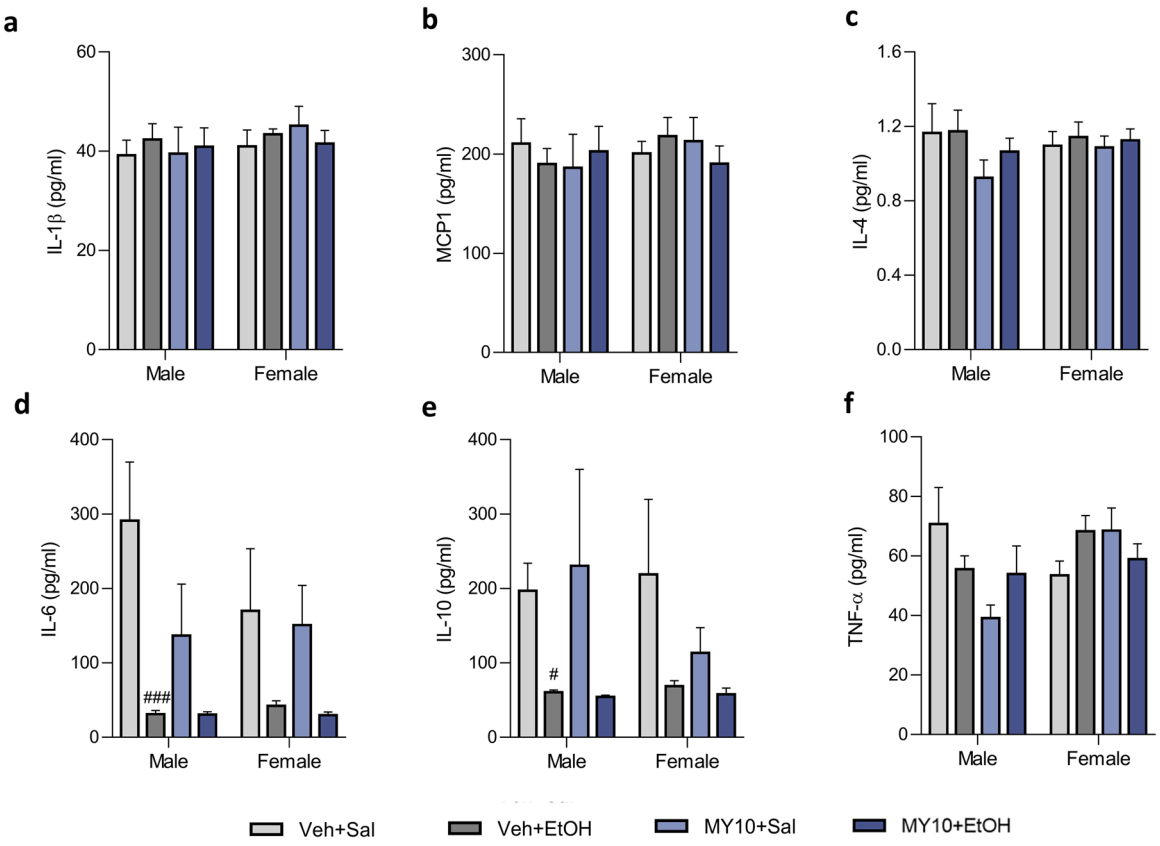

Fig. 6. Effects of MY10 and ethanol on cytokine circulating levels in adolescent mice. IL-1β, MCP-1, IL-4, IL-6, IL-10 and TNF-α protein levels measured using a Milliplex system in plasma samples of vehicle+saline (Veh+Sal)-, vehicle+ethanol (Veh+EtOH)-, MY10 +saline (MY10 +Sal)- and MY10 +ethanol (MY10 +EtOH)-treated animals (n = 5–6/group/sex) extracted 1 h after ethanol or saline treatment. # $P < 0.05$; ### $P < 0.001$ vs. male vehicle+saline.

of this study is that the effects of ethanol in the brain were only analyzed at one time point. We cannot exclude the possibility that previous changes in glial responses impact the loss of hippocampal neurogenesis observed eighteen hours after ethanol administration.

Treatment with MY10 did not show modulatory effects on ethanol-induced changes in none of the circulating cytokines tested. However, surprisingly, treatment with MY10 alone reduced circulating levels of TNF-α only in male mice, suggesting sex differences in the contribution of RPTPβ/ζ to the regulation of basal immune states. Overall, these results point to the existence of sex differences in the phosphatase activity of RPTPβ/ζ that are relevant to ethanol-induced neuroimmune responses and may be important in other physiological and pathological conditions. Additional studies are needed to confirm this possibility.

The exact molecular mechanisms involved in the prevention of ethanol-induced reduction of hippocampal neurogenesis by the inhibition of RPTPβ/ζ remain to be studied. However, it is interesting to note that known substrates of this receptor play relevant roles in preventing impairments of neurogenesis in other contexts. TrkA is one substrate whose phosphorylation levels in Tyr residues, critical for the activation of its kinase activity, are increased after inhibition of RPTPβ/ζ with PTN or MY10 (Fernández-Calle et al., 2018b). Importantly, activation of the TrkA signaling pathway plays a critical role in reducing radiotherapy-induced impairments in neurogenesis (Ji et al., 2020). Similarly, the function of ALK, another substrate of RPTPβ/ζ, is important for the preservation of hippocampal neurogenesis (Weiss et al., 2012). Again, inhibition of RPTPβ/ζ with MY10 results in increased phosphorylation of key Tyr residues in ALK for the activation of its kinase activity (Fernández-Calle et al., 2018b). Thus, it is tempting to speculate that MY10 may prevent ethanol-induced decrease of hippocampal neurogenesis by its ability to activate TrkA and ALK through inhibition of RPTPβ/ζ.

5. Conclusions

In summary, we have identified a novel mechanism that regulates the loss of hippocampal neurogenesis induced by ethanol in the brain of adolescent male and female mice. Pharmacological inhibition of the phosphatase activity of RPTPβ/ζ fully prevents this critical detrimental effect of ethanol in the adolescent brain. In addition, our studies suggest that RPTPβ/ζ function may be important for immune responses and for ethanol-induced glial responses in a sex-dependent manner.

Funding sources

This work was supported by National Plan on Drug Abuse, Ministerio de Sanidad of Spain (MSSSI, grant PNSD2019I015 to G.H.) and by ISCIII-Redes de Investigación Cooperativa Orientadas a Resultados en Salud (RICORS), Red de Investigación en Atención Primaria de Adicciones (RIAPAd; grant RD21/0009/0013 to G.H.).

CRediT authorship contribution statement

M. Galán-Llario, M. Rodríguez-Zapata, T. Fontán-Baselga, M.C. Ovejero-Benito, J. Carrasco, M. Moreno-Herradón, J.M. Zapico: Investigation, Data curation, Visualization. **E. Gramage, M. Vicente-Rodríguez, C. Pérez-García, J. Sevillano:** Conceptualization, Investigation, Methodology, Supervision, Writing – review & editing. **M.P. Ramos-Álvarez, B. Pascual-Teresa, A. Ramos:** Resources, Writing – review & editing, Funding acquisition. **G. Herradón:** Conceptualization, Writing – review & editing, Funding acquisition, Project administration.

Declaration of Competing Interest

The authors declare that they have no known competing financial interests or personal relationships that could have appeared to influence the work reported in this paper.

Data availability

Data will be made available on request.

Acknowledgments

We thank our colleagues in the Animal facility and the "Instituto de Medicina Molecular Aplicada" (IMMA) in the Universidad CEU San Pablo.

Appendix A. Supporting information

Supplementary data associated with this article can be found in the online version at doi:10.1016/j.neuro.2022.11.008.

References

Anacker, C., Hen, R., 2017. Adult hippocampal neurogenesis and cognitive flexibility - linking memory and mood. Nat. Rev. Neurosci. 18, 335–346.
Bilbo, S.D., Smith, S.H., Schwarz, J.M., 2012. A lifespan approach to neuroinflammatory and cognitive disorders: a critical role for glia. J. NeuroImmune Pharmacol.: Off. J. Soc. NeuroImmune Pharmacol. 7, 24–41.
Bollinger, J.L., 2021. Uncovering microglial pathways driving sex-specific neurobiological effects in stress and depression. Brain, Behav., Immun. - Health 16, 100320.
Broadwater, M.A., Liu, W., Crews, F.T., Spear, L.P., 2014. Persistent loss of hippocampal neurogenesis and increased cell death following adolescent, but not adult, chronic ethanol exposure. Dev. Neurosci. 36, 297–305.
Calleja-Conde, J., Fernández-Calle, R., Zapico, J.M., Ramos, A., de Pascual-Teresa, B., Bühler, K.M., Echeverry-Alzate, V., Giné, E., Rodríguez de Fonseca, F., López-Moreno, J.A., Herradón, G., 2020. Inhibition of Receptor Protein Tyrosine Phosphatase β/ζ Reduces Alcohol Intake in Rats. Alcohol Clin. Exp. Res 44, 1037–1045.
Coleman Jr., L.G., Crews, F.T., 2018. Innate immune signaling and alcohol use disorders. Handb. Exp. Pharmacol. 248, 369–396.
Cressant, A., Dubreuil, V., Kong, J., Kranz, T.M., Lazarini, F., Launay, J.M., Callebert, J., Sap, J., Malaspina, D., Granon, S., Harroch, S., 2017. Loss-of-function of PTPR γ and ζ, observed in sporadic schizophrenia, causes brain region-specific deregulation of monoamine levels and altered behavior in mice. Psychopharmacol. (Berl.) 234, 575–587.
Del Campo, M., Fernández-Calle, R., Vicente-Rodríguez, M., Martín Martínez, S., Gramage, E., Zapico, J.M., Haro, M., Herradon, G., 2021. Role of receptor protein tyrosine phosphatase β/ζ in neuron-microglia communication in a cellular model of Parkinson's disease. Int. J. Mol. Sci. **22**.
Dutton 3rd, J.W., Chen, H., You, C., Brodie, M.S., Lasek, A.W., 2017. Anaplastic lymphoma kinase regulates binge-like drinking and dopamine receptor sensitivity in the ventral tegmental area. Addict. Biol. 22, 665–678.
Fernández-Calle, R., Vicente-Rodríguez, M., Gramage, E., Pita, J., Pérez-García, C., Ferrer-Alcón, M., Uribarri, M., Ramos, M.P., Herradón, G., 2017. Pleiotrophin regulates microglia-mediated neuroinflammation. J. Neuroinflamm. 14, 46.
Fernández-Calle, R., Vicente-Rodríguez, M., Gramage, E., de la Torre-Ortiz, C., Pérez-García, C., Ramos, M.P., Herradón, G., 2018a. Endogenous pleiotrophin and midkine regulate LPS-induced glial responses. Neurosci. Lett. 662, 213–218.
Fernández-Calle, R., Vicente-Rodríguez, M., Pastor, M., Gramage, E., Di Geronimo, B., Zapico, J.M., Coderch, C., Pérez-García, C., Lasek, A.W., de Pascual-Teresa, B., Ramos, A., Herradón, G., 2018b. Pharmacological inhibition of Receptor Protein Tyrosine Phosphatase β/ζ (PTPRZ1) modulates behavioral responses to ethanol. Neuropharmacology 137, 86–95.
Fernández-Calle, R., Gramage, E., Zapico, J.M., de Pascual-Teresa, B., Ramos, A., Herradón, G., 2019. Inhibition of RPTPβ/ζ blocks ethanol-induced conditioned place preference in pleiotrophin knockout mice. Behav. Brain Res 369, 111933.
Fernández-Calle, R., Galán-Llario, M., Gramage, E., Zapatería, B., Vicente-Rodríguez, M., Zapico, J.M., de Pascual-Teresa, B., Ramos, A., Ramos-Álvarez, M.P., Uribarri, M., Ferrer-Alcón, M., Herradón, G., 2020. Role of RPTPβ/ζ in neuroinflammation and microglia-neuron communication. Sci. Rep. 10, 20259.
Guerri, C., Pascual, M., 2019. Impact of neuroimmune activation induced by alcohol or drug abuse on adolescent brain development. Int. J. Dev. Neurosci.: Off. J. Int. Soc. Dev. Neurosci. 77, 89–98.
Harroch, S., Furtado, G.C., Brueck, W., Rosenbluth, J., Lafaille, J., Chao, M., Buxbaum, J. D., Schlessinger, J., 2002. A critical role for the protein tyrosine phosphatase receptor type Z in functional recovery from demyelinating lesions. Nat. Genet. 32, 411–414.
Herradon, G., Ezquerra, L., 2009. Blocking receptor protein tyrosine phosphatase beta/zeta: a potential therapeutic strategy for Parkinson's disease. Curr. Med Chem. 16, 3322–3329.
Herradon, G., Ramos-Alvarez, M.P., Gramage, E., 2019. Connecting Metainflammation and Neuroinflammation Through the PTN-MK-RPTPβ/ζ Axis: Relevance in Therapeutic Development. Front. Pharmacol. 10, 377.
Herradón, G., Pérez-García, C., 2014. Targeting midkine and pleiotrophin signalling pathways in addiction and neurodegenerative disorders: recent progress and perspectives. Br. J. Pharm. 171, 837–848.
Ji, S., Wu, H., Ding, X., Chen, Q., Jin, X., Yu, J., Yang, M., 2020. Increased hippocampal TrkA expression ameliorates cranial radiation-induced neurogenesis impairment and cognitive deficit via PI3K/AKT signaling. Oncol. Rep. 44, 2527–2536.
Lamprianou, S., Chatzopoulou, E., Thomas, J.L., Bouyain, S., Harroch, S., 2011. A complex between contactin-1 and the protein tyrosine phosphatase PTPRZ controls the development of oligodendrocyte precursor cells. Proc. Natl. Acad. Sci. USA 108, 17498–17503.
Lisdahl, K.M., Gilbart, E.R., Wright, N.E., Shollenbarger, S., 2013. Dare to delay? The impacts of adolescent alcohol and marijuana use onset on cognition, brain structure, and function. Front Psychiatry 4, 53.
López-Sánchez, N., Frade, J.M., 2013. Genetic evidence for p75NTR-dependent tetraploidy in cortical projection neurons from adult mice. J. Neurosci. 33, 7488–7500.
López-Sánchez, N., Fontán-Lozano, Á., Pallé, A., González-Álvarez, V., Rábano, A., Trejo, J.L., Frade, J.M., 2017. Neuronal tetraploidization in the cerebral cortex correlates with reduced cognition in mice and precedes and recapitulates Alzheimer's-associated neuropathology. Neurobiol. Aging 56, 50–66.
Macht, V., Crews, F.T., Vetreno, R.P., 2020. Neuroimmune and epigenetic mechanisms underlying persistent loss of hippocampal neurogenesis following adolescent intermittent ethanol exposure. Curr. Opin. Pharmacol. 50, 9–16.
Meng, K., Rodriguez-Pena, A., Dimitrov, T., Chen, W., Yamin, M., Noda, M., Deuel, T.F., 2000. Pleiotrophin signals increased tyrosine phosphorylation of beta beta-catenin through inactivation of the intrinsic catalytic activity of the receptor-type protein tyrosine phosphatase beta/zeta. Proc. Natl. Acad. Sci. USA 97, 2603–2608.
Meredith, L.R., Burnette, E.M., Grodin, E.N., Irwin, M.R., Ray, L.A., 2021. Immune treatments for alcohol use disorder: A translational framework. Brain, Behav., Immun. 97, 349–364.
Nagai, K., Fujii, M., Kitazume, S., 2022. Protein Tyrosine Phosphatase Receptor Type Z in Central Nervous System Disease. Int J. Mol. Sci. 23, 4414.
Orio, L., Antón, M., Rodríguez-Rojo, I.C., Correas, Á., García-Bueno, B., Corral, M., de Fonseca, F.R., García-Moreno, L.M., Maestú, F., Cadaveira, F., 2018. Young alcohol binge drinkers have elevated blood endotoxin, peripheral inflammation and low cortisol levels: neuropsychological correlations in women. Addict. Biol. 23, 1130–1144.
Papadimitriou, E., Mourkogianni, E., Ntenekou, D., Christopoulou, M., Koutsioumpa, M., Lamprou, M., 2022. On the role of pleiotrophin and its receptors in development and angiogenesis. Int J. Dev. Biol. 66, 115–124.
Pariser, H., Ezquerra, L., Herradon, G., Perez-Pinera, P., Deuel, T.F., 2005a. Fyn is a downstream target of the pleiotrophin/receptor protein tyrosine phosphatase beta/zeta-signaling pathway: regulation of tyrosine phosphorylation of Fyn by pleiotrophin. Biochem Biophys. Res Commun. 332, 664–669.
Pariser, H., Herradon, G., Ezquerra, L., Perez-Pinera, P., Deuel, T.F., 2005b. Pleiotrophin regulates serine phosphorylation and the cellular distribution of beta-adducin through activation of protein kinase C. Proc. Natl. Acad. Sci. USA 102, 12407–12412.
Pariser, H., Perez-Pinera, P., Ezquerra, L., Herradon, G., Deuel, T.F., 2005c. Pleiotrophin stimulates tyrosine phosphorylation of beta-adducin through inactivation of the transmembrane receptor protein tyrosine phosphatase beta/zeta. Biochem Biophys. Res Commun. 335, 232–239.
Pascual, M., Baliño, P., Aragón, C.M., Guerri, C., 2015. Cytokines and chemokines as biomarkers of ethanol-induced neuroinflammation and anxiety-related behavior: role of TLR4 and TLR2. Neuropharmacology 89, 352–359.
Pascual, M., Montesinos, J., Guerri, C., 2018. Role of the innate immune system in the neuropathological consequences induced by adolescent binge drinking. J. Neurosci. Res. 96, 765–780.
Pascual, M., López-Hidalgo, R., Montagud-Romero, S., Ureña-Peralta, J.R., Rodríguez-Arias, M., Guerri, C., 2021. Role of mTOR-regulated autophagy in spine pruning defects and memory impairments induced by binge-like ethanol treatment in adolescent mice. Brain Pathol. (Zur., Switz.) 31, 174–188.
Pastor, M., Fernández-Calle, R., Di Geronimo, B., Vicente-Rodríguez, M., Zapico, J.M., Gramage, E., Coderch, C., Pérez-García, C., Lasek, A.W., Puchades-Carrasco, L., Pineda-Lucena, A., de Pascual-Teresa, B., Herradón, G., Ramos, A., 2018. Development of inhibitors of receptor protein tyrosine phosphatase β/ζ (PTPRZ1) as candidates for CNS disorders. Eur. J. Med. Chem. 144, 318–329.
Posillico, C.K., 2021. Three's Company: Neuroimmune activation, sex, and memory at the tripartite synapse. Brain, Behav., Immun. - Health 16, 100326.
Pruett, S., Tan, W., Howell III, G.E., Nanduri, B., 2020. Dosage scaling of alcohol in binge exposure models in mice: An empirical assessment of the relationship between dose, alcohol exposure, and peak blood concentrations in humans and mice. Alcohol 89, 9e17.
Ron, D., Berger, A., 2018. Targeting the intracellular signaling "STOP" and "GO" pathways for the treatment of alcohol use disorders. Psychopharmacol. (Berl.) 235, 1727–1743.
Snyder, J.S., 2019. Recalibrating the relevance of adult neurogenesis. Trends Neurosci. 42, 164–178.

Swartzwelder, H.S., Healey, K.L., Liu, W., Dubester, K., Miller, K.M., Crews, F.T., 2019. Changes in neuroimmune and neuronal death markers after adolescent alcohol exposure in rats are reversed by Donepezil. Sci. Rep. 9, 12110.
Vetreno, R.P., Lawrimore, C.J., Rowsey, P.J., Crews, F.T., 2018. Persistent adult neuroimmune activation and loss of hippocampal neurogenesis following adolescent ethanol exposure: blockade by exercise and the anti-inflammatory drug indomethacin. Front. Neurosci. 12, 200.
Vicente-Rodriguez, M., Perez-Garcia, C., Ferrer-Alcon, M., Uribarri, M., Sanchez-Alonso, M.G., Ramos, M.P., Herradon, G., 2014. Pleiotrophin differentially regulates the rewarding and sedative effects of ethanol. J. Neurochem 131, 688–695.
Vicente-Rodríguez, M., Rojo Gonzalez, L., Gramage, E., Fernández-Calle, R., Chen, Y., Pérez-García, C., Ferrer-Alcón, M., Uribarri, M., Bailey, A., Herradón, G., 2016. Pleiotrophin overexpression regulates amphetamine-induced reward and striatal dopaminergic denervation without changing the expression of dopamine D1 and D2 receptors: Implications for neuroinflammation. Eur. Neuropsychopharmacol.: J. Eur. Coll. Neuropsychopharmacol. 26, 1794–1805.
Weiss, J.B., Xue, C., Benice, T., Xue, L., Morris, S.W., Raber, J., 2012. Anaplastic lymphoma kinase and leukocyte tyrosine kinase: functions and genetic interactions in learning, memory and adult neurogenesis. Pharm. Biochem Behav. 100, 566–574.
Wiener, S.W., Olmedo, R., Howland, M., Nelson, L., Hoffman, R., 2013. Ethanol elimination kinetics following massive ingestion in an ethanol naive child. Hum. Exp. Toxicol. 32, 775e777.
Winner, B., Winkler, J., 2015. Adult neurogenesis in neurodegenerative diseases. Cold Spring Harb. Perspect. Biol. 7, a021287.
Yttri, E.A., Burk, J.A., Hunt, P.S., 2004. Intermittent ethanol exposure in adolescent rats: dose-dependent impairments in trace conditioning. Alcohol Clin. Exp. Res 28, 1433–1436.
Zapata, A., Gonzales, R.A., Shippenberg, T.S., 2006. Repeated ethanol intoxication induces behavioral sensitization in the absence of a sensitized accumbens dopamine response in C57BL/6J and DBA/2J mice. Neuropsychopharmacology 31, 396–405.